Parton Distribution Function from the Hadronic Tensor on the Lattice

Keh-Fei Liu[*]

Dept. of Physics and Astronomy,University of Kentucky, Lexington, KY 40506, USA
E-mail: liu@pa.uky.edu

The path-integral formulation of the hadronic tensor $W_{\mu\nu}$ of deep inelastic scattering is reviewed. It is shown that there are 3 gauge invariant and topologically distinct contributions. The separation of the connected sea partons from those of the disconnected sea can be achieved with a combination of the global fit of the parton distribution function (PDF), the semi-inclusive DIS data on the strange PDF and the lattice calculation of the ratio of the strange to u/d momentum fraction in the disconnected insertion.

We shall discuss numerical issues associated with lattice calculation of the hadronic tensor involving a four-point function, such as large hadron momenta and improved maximum entropy method to obtain the spectral density from the hadronic tensor in Euclidean time.

We also draw a comparison between the large momentum approach to the parton distribution function (PDF) and the hadronic tensor approach.

---

[*]Speaker.

1. Hadronic tensor in path-integral formulism

The deep inelastic scattering of a muon on a nucleon involves the hadronic tensor which, being an inclusive reaction, includes all intermediate states

$$W_{\mu\nu}(q^2,\nu) = \frac{1}{2}\sum_n \int \prod_{i=1}^n \left[\frac{d^3 p_i}{(2\pi)^3 2E_{pi}}\right] \langle N|J_\mu(0)|n\rangle \langle n|J_\nu(0)|N\rangle_{spin\,ave.}(2\pi)^3 \delta^4(p_n - p - q). \quad (1.1)$$

Since deep inelastic scattering measures the absorptive part of the Compton scattering, it is the imaginary part of the forward amplitude and can be expressed as the current-current correlation function in the nucleon, i.e.

$$W_{\mu\nu}(q^2,\nu) = \frac{1}{\pi}\mathrm{Im}T_{\mu\nu}(q^2,\nu) = \langle N|\int \frac{d^4 x}{4\pi}e^{iq\cdot x}J_\mu(x)J_\nu(0)|N\rangle_{spin\,ave.}. \quad (1.2)$$

It has been shown [1, 2, 3, 4, 5] that the hadronic tensor $W_{\mu\nu}(q^2,\nu)$ can be obtained from the Euclidean path-integral formalism. In this case, one considers the ratio of the four-point function $\langle \chi_N(\vec{p},t)\int \frac{d^3 x}{4\pi}e^{-i\vec{q}\cdot\vec{x}}J_\nu(\vec{x},t_2)J_\mu(0,t_1)\chi_N(\vec{p},t_0)\rangle$ and the two-point function $\langle \chi_N(\vec{p},t)\chi_N(\vec{p},t_0)\rangle$, where $\chi_N(\vec{p},t)$ is an interpolation field for the nucleon with momentum p at Euclidean time t.

As both $t - t_2 \gg 1/\Delta E_p$ and $t_1 - t_0 \gg 1/\Delta E_p$, where ΔE_p is the energy gap between the nucleon energy E_p and the next excitation (i.e. the threshold of a nucleon and a pion in the p-wave), the intermediate state contributions from the interpolation fields will be dominated by the nucleon with the Euclidean propagator $e^{-E_p(t-t_0)}$. From the three-point and two-point functions on the lattice

$$G_{pWp}^{\alpha\beta} = \sum_{\vec{x}_f}e^{-i\vec{p}\cdot\vec{x}_f}\left\langle \chi_N^\alpha(\vec{x}_f,t)\sum_{\vec{x}}\frac{e^{-i\vec{q}\cdot\vec{x}}}{4\pi}J_\mu(\vec{x},t_2)J_\nu(0,t_1)\sum_{\vec{x}_0}e^{i\vec{p}\cdot\vec{x}_0}\overline{\chi}_N^\beta(\vec{x}_0,t_0)\right\rangle, \quad (1.3)$$

$$G_{pp}^{\alpha\beta} = \sum_{\vec{x}_f}e^{-i\vec{p}\cdot\vec{x}_f}\left\langle \chi_N^\alpha(\vec{x}_f,t)\overline{\chi}_N^\beta(\vec{x}_0=0,t_0)\right\rangle, \quad (1.4)$$

we define

$$\begin{aligned}
\widetilde{W}_{\mu\nu}(\vec{q},\vec{p},\tau) &= \left.\frac{E_p}{m_N}\frac{\mathrm{Tr}(\Gamma_e G_{pWp})}{\mathrm{Tr}(\Gamma_e G_{pp})}\right|_{t-t_2\gg 1/\Delta E_p,\,t_1-t_0\gg 1/\Delta E_p} \\
&= \frac{E_p}{m_N}\frac{\frac{|Z|^2 m_N(E_p+m_N)}{E_p^2}e^{-E_p(t-t_0)}<N|\sum_{\vec{x}}\frac{e^{-i\vec{q}\cdot\vec{x}}}{4\pi}J_\mu(\vec{x},t_2)J_\nu(0,t_1)|N>}{\frac{|Z|^2(E_p+m_N)}{E_p}e^{-E_p(t-t_0)}} \\
&= <N|\sum_{\vec{x}}\frac{e^{i\vec{q}\cdot\vec{x}}}{4\pi}e^{-i\vec{q}\cdot\vec{x}}J_\mu(\vec{x},\tau)J_\nu(0,0)|N>, \quad (1.5)
\end{aligned}$$

where $\tau = t_2 - t_1$, Z is the transition matrix element $\langle 0|\chi_N|N\rangle$, and $\Gamma_e = \frac{1+\gamma_4}{2}$ is the unpolarized projection to the positive parity nucleon state. Inserting intermediate states, $\widetilde{\widetilde{W}}_{\mu\nu}(\vec{q}^2,\tau)$ becomes

$$\widetilde{W}_{\mu\nu}(\vec{q}^2,\tau) = \frac{1}{4\pi}\sum_n\left(\frac{2m_N}{2E_n}\right)\delta_{\vec{p}+\vec{q},\vec{p}_n}\langle N(p)|J_\mu(0)|n\rangle \langle n|J_\nu(0)|N(p)\rangle_{spin\,ave.}e^{-(E_n-E_p)\tau}. \quad (1.6)$$

2

Formally, to recover the delta function $\delta(E_n - E_p + \nu)$ in Eq. (1.1) in the continuum formalism, one can carry out the inverse Laplace transform with τ being treated as a dimensionful continuous variable

$$W_{\mu\nu}(q^2,\nu) = \frac{1}{2m_N i} \int_{c-i\infty}^{c+i\infty} d\tau\, e^{\nu\tau} \widetilde{W}_{\mu\nu}(\vec{q}^2,\tau), \tag{1.7}$$

with $c > 0$. This is basically doing the anti-Wick rotation back to the Minkowski space. We will discuss the numerical lattice approach to this conversion from Euclidean space to Minkowski space later.

2. Parton degrees of freedom

In addressing the origin of the Gottfried sum rule violation, it is shown [1, 2, 3] that the contributions to the four-point function of the Euclidean path-integral formulation of the hadronic tensor $\widetilde{W}_{\mu\nu}(\vec{q}^2,\tau)$ in Eq. (1.6) can be classified according to different topologies of the quark paths between the source and the sink of the proton. Fig. 1(a) and 1(b) represent connected insertions (C.I.) of the currents. Here the quark fields from the interpolators χ_N contract with the currents such that the quark lines flow continuously from $t = 0$ to $t = t$. Fig. 1(c), on the other hand, represents a disconnected insertion (D.I.) where the quark fields from J_μ and J_ν self-contract and, as a consequence, the quark loop is disconnected from the quark paths between the proton source and sink. Here, "disconnected" refers only to the quark lines. Of course, quarks dive in the background of the gauge field and all quark paths are ultimately connected through the gluon field.
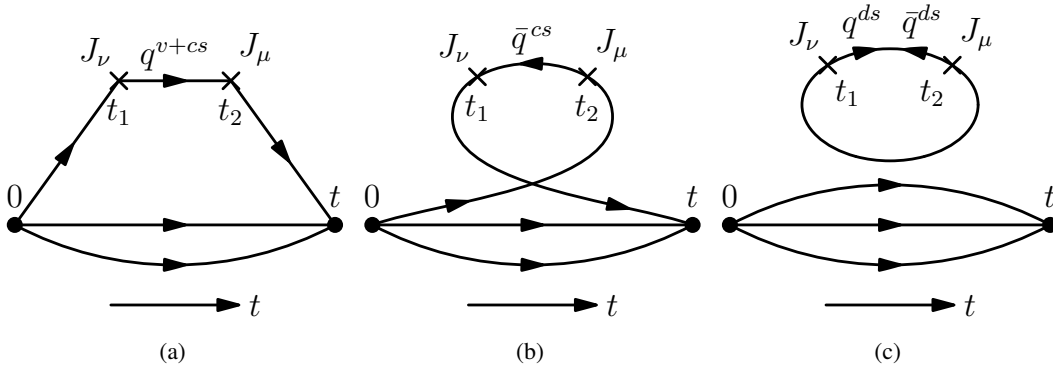

Figure 1: Three gauge invariant and topologically distinct diagrams in the Euclidean-path integral formulation of the nucleon hadronic tensor in the large momentum frame. In between the currents at t_1 and t_2, the parton degrees of freedom are (a) the valence and connected sea (CS) partons q^{v+cs}, (b) the CS anti-partons $\bar{q}^{cs}$. Only u and d are present in (a) and (b) for the nucleon hadronic tensor. (c) the disconnected sea (DS) partons q^{ds} and anti-partons $\bar{q}^{ds}$ with $q = u, d, s$, and c.

We first note that Fig. 1(b), where the quarks propagate backward in time between t_1 and t_2 corresponds to the connected sea (CS) anti-partons $\bar{u}^{cs}$ and $\bar{d}^{cs}$, since the quark lines are connected to the nucleon interpolation fields at $t = 0$ and $t = t$. By the same token, Fig. 1(a) gives the valence and CS partons u^{v+cs} and d^{v+cs}, and the valence is defined as $u^v(d^v) \equiv u^{v+cs}(d^{v+cs}) - \bar{u}^{cs}(\bar{d}^{cs})$ and $u^{cs}(x) \equiv \bar{u}^{cs}(x)$. On the other hand, Fig. 1(c) gives the disconnected sea (DS) q^{ds} and $\bar{q}^{ds}$ with $\{q = u, d, s, c\}$. We see that while u and d have both CS and DS, strange and charm have only DS.

3

It is clear from these diagrams that there are two sources of the sea partons, one is CS and the other is DS. In the isospin limit where $\bar{u}^{ds}(x) = \bar{d}^{ds}(x)$, the DS do not contribute to the Gottfried sum rule (GSR) violation which reveals that $\int_0^1 dx[\bar{u}(x) - \bar{d}(x)] < 0$ from DIS experiments. The isospin symmetry breaking due to the u and d mass difference should be of the order of $(m_d - m_u)/m_N$ and cannot explain the large violation of GSR. Rather, the majority of the violation should come from the CS.

As far as the small-x behavior is concerned, there is only reggeon exchange for the flavor non-singlet valence and CS, so the small-x behavior for the valence and CS partons is $q^{v+cs}(x), \bar{q}^{cs}(x) \underset{x\to 0}{\to} \propto x^{-1/2}$. On the other hand, there is flavor-singlet pomeron exchange in addition to the reggeon exchange for the singlet DS partons, thus its small x behavior is more singular, i.e. $q^{ds}(x), \bar{q}^{ds}(x) \underset{x\to 0}{\to} \propto x^{-1}$.

In the global fittings of parton distribution function (PDF), the CS is not separated from the DS and it had been implicitly assumed that all the anti-partons are from the DS. That's why the GSR violation came as a surprise and the fitting has accommodated the $\bar{u}(x) - \bar{d}(x)$ difference from experiment. However, it is still mostly assumed that the $\bar{u}(x) + \bar{d}(x)$ has the same x dependence as that of $s(x) + \bar{s}(x)$. As we discussed above, $\bar{u}(x) + \bar{d}(x) = \bar{u}^{cs}(x) + \bar{d}^{cs}(x) + \bar{u}^{ds}(x) + \bar{d}^{ds}(x)$ have both the CS and DS partons and they have different small x behaviors. This is in contrast to $s(x) + \bar{s}(x)$ where there are only DS partons. Combining HERMES data on the strangeness parton distribution [6], the CT10 global fitting of the $\bar{u}(x) + \bar{d}(x)$ distributions [7], and the lattice result of the moment ratio of the strange to u/d in the disconnected insertion, i.e. $\langle x \rangle_{s+\bar{s}}/\langle x \rangle_{u+\bar{u}}(\text{DI})$ [8], it is demonstrated [9] that the CS and DS partons can be separated and the CS $\bar{u}^{cs}(x) + \bar{d}^{cs}(x)$ distribution of the proton is obtained in the region $0.03 < x < 0.4$ at $Q^2 = 2.5$ GeV^2. This assumes that the distribution of $\bar{u}^{ds}(x) + \bar{d}^{ds}(x)$ is proportional to that of $s(x) + \bar{s}(x)$, so that the CS partons can be extracted at $Q^2 = 2.5$ GeV^2 through the relation

$$\bar{u}^{cs}(x) + \bar{d}^{cs}(x) = \bar{u}(x) + \bar{d}(x) - \frac{1}{R}(s(x) + \bar{s}(x)), \tag{2.1}$$

where $(s(x) + \bar{s}(x))$ is from the HERMES experiment [6], $\bar{u}(x) + \bar{d}(x)$ is from the CT10 gobal fitting of PDF [7], and R is defined as

$$R = \frac{\langle x \rangle_{s+\bar{s}}}{\langle x \rangle_{u+\bar{u}}(DI)}, \tag{2.2}$$

and we have used the lattice result $R = 0.857(40)$ [8] for the extraction.

The results of $x(\bar{u}(x) + \bar{d}(x) - \frac{1}{R}(s(x) + \bar{s}(x)))$, $x(\bar{u}^{ds}(x) + \bar{d}^{ds}(x) = \frac{1}{R}x(s(x) + \bar{s}(x)))$ and $x(\bar{u}(x) + \bar{d}(x))$ from CT10 in Fig. 2 are plotted in Fig. 2 to show that the CS and DS have very different x-dependence.

The extraction of $\bar{u}^{cs}(x) + \bar{d}^{cs}(x)$ in Eq. (2.1) is based on the assumption that the distribution of $s(x) + \bar{s}(x)$ is proportional to that of $u^{ds}(x) + \bar{u}^{ds}(x)$ or $d^{ds}(x) + \bar{d}^{ds}(x)$ so that their ratio can be obtained via the ratio R in Eq. (2.2). It would be better to calculate the disconnected insertion of $W_{\mu\nu}$ represented in Fig. 1(c) directly on the lattice.

There is a persistent tension between the lattice calculation of the second moment of $u - d$ and that of the global fitting [10, 11]. The PDF data is from $\langle x \rangle_{u-d} = \langle x(u(x) - d(x)) \rangle$ which, according to the path-integral classification, corresponds to $\langle x(u^{v+cs}(x) - d^{v+cs}(x)) \rangle + \langle x(\bar{u}^{cs}(x) - \bar{d}^{cs}(x)) \rangle$. Thus, it is desirable to calculate the $u^{v+cs}(x)(d^{v+cs}(x))$ from Fig. 1(a) and CS in Fig. 1(b) to check the Gottfried sum rule violation directly and address the discrepancy of the second moment.
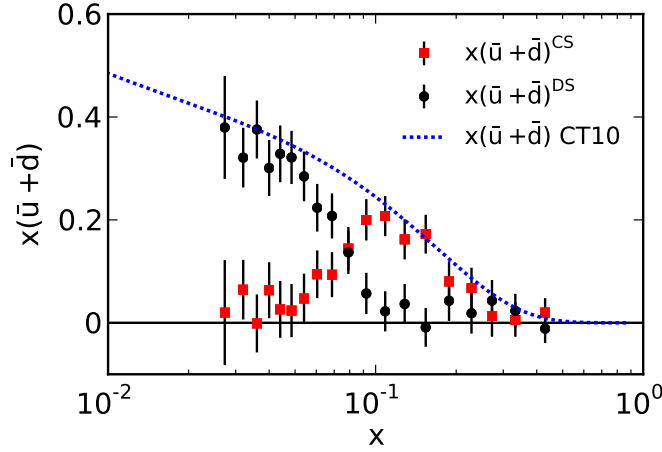
4

Figure 2: The $x(\bar{d}^{cs}(x) + \bar{u}^{cs}(x))$ as obtained from Eq. (2.1) is plotted together with $x(\bar{d}(x) + \bar{u}(x))$ from CT10 and $\frac{1}{R}x(s(x) + \bar{s}(x))$ which is taken to be $x(u^{ds}(x) + \bar{u}^{ds}(x))$.

3. Numeral calculation on the lattice

The calculation of Euclidean hadronic tensor $\widetilde{W}_{\mu\nu}(\vec{q}, \vec{p}, \tau)$, which involves four-point functions, entails two sequential inversions which is somewhat more complicated than the three-point function calculations for the nucleon form factors and parton moments. Furthermore, the large momentum transfer $|\vec{q}| \gg m_N$ and large energy transfer $\nu = E_n - E_p$, which are needed to sustain the parton interpretation, are challenges for the lattice calculation as they will require fine lattice spacings. The small Bjorken $x = \frac{Q^2}{2(E_p\nu - \vec{p}\cdot\vec{q})}$ can be accessed with a non-zero nucleon momentum $|\vec{p}|$ which is antiparallel to $\vec{q}$. For example, with $\vec{q} = -\vec{p}$ ($|\vec{q}| = |\vec{p}| = 3$ GeV), and $Q^2 = 2\,\mathrm{GeV}^2$, the Bjorken x is 0.058. As can be seen in Fig. 2, this x should be low enough to discern the difference between $x(\bar{u}^{cs} + \bar{d}^{cs})$ and $x(\bar{u}^{ds} + \bar{d}^{ds})$. There are applications where lattice calculations require large hadron momenta, such as the semi-leptonic decays of heavy meson $B \to \pi\ell\bar{\nu}_\ell$ and heavy baryon $\Lambda_b \to p\ell\bar{\nu}_\ell$ [12], and the large momentum approach to calculating TMD [13, 14, 15] and PDF [16]. In view of this, there have been several studies to address this issue on the lattice [17, 18, 19].

The most challenging and critical task is to convert the $\widetilde{W}_{\mu\nu}$ on the Euclidean lattice in Eq. (1.5) to the hadronic tensor $W_{\mu\nu}$ in the Minkowski space. The inverse Laplace transform in Eq. (1.7) is ture only formally but not practical, since there are no lattice data for imaginary τ. Naively, one may attempt to consider using $\lim_{\varepsilon \to \infty} \int_0^{\tau_{max}} d\tau e^{(\nu + i\varepsilon)\tau} \widetilde{W}_{\mu\nu}(\vec{q}^2, \tau)$ to pick out the delta function $\delta(\nu - (E_n - E_p))$ to complete the 4-D delta function in Eq. (1.1). However, this introduces an exponentially function $e^{(\nu - E_m + E_p)\tau} = e^{(E_n - E_m)\tau}$ in the integrand for $E_m \neq E_n$. For those intermediate states lower than E_n, i.e. $E_m < E_n$, they will have exponentially increasing contributions compared to the constant δ-function that one is trying to pull out [20]. This will not work for DIS where the virtuality is large, i.e. $\nu \gg m_N$.

$W_{\mu\nu}(q^2, \nu)$ is just the spectral density $\rho(\omega)$ with the excitation energy $\omega = \nu$. The task is to solve the inverse problem in order to find the spectral density $\rho(\omega)$ from its spectral representation

in the integral

$$D(\tau) = \int K(\tau, \omega) \rho(\omega) d\omega \qquad (3.1)$$

where $D(\tau) = \widetilde{W}_{\mu\nu}(\tau)$ and the kernel $K(\tau, \omega) = e^{-\omega\tau}$. A common approach to this inverse problem is the Maximum Entropy Method (MEM) [21]. Bayes' theorem $P[\rho|D,I] = \frac{P[D|\rho,I]P[\rho|I]}{P[D|I]}$, where $P[D|\rho,I] \propto e^{-L}$ is the likelihood probability with $L = \frac{1}{2}\chi^2$ being the χ^2 for the theoretical model with the discrete version of the spectral representation $D_\rho(\tau_i) = \sum_{\ell=1}^{N_\omega} e^{-\omega_\ell \tau_i} \rho_\ell \Delta\omega_\ell$. The standard MEM is to find ρ_ℓ to maximize $P[\rho|D,I] \propto e^{\alpha S - L}$ where S is the Shannon-Jaynes information entropy. Recently, there is an improved MEM which can lead to more stable fit [22]. The improved probability to maximize is

$$P[\rho|D,I] \propto e^{\alpha S - L - \gamma(L - N_\tau)^2}, \qquad (3.2)$$

where N_τ is the number of τ_i and S is modified to $S = \int d\omega [1 - \rho(\omega)/m(\omega) - \ln(\rho(\omega)/m(\omega))]$. Given this new promising approach to the inverse problem, it is worthwhile to tackle the hadronic tensor $W_{\mu\nu}$ calculation on the lattice. It does require precise data for the improved MEM, however.

4. Comparison with the large momentum approach to calculating PDF

There is another approach to calculating PDF on lattice proposed by Xiangdong Ji [16]. The idea is to calculate the 'quasiparton' $\tilde{q}(x, \Lambda, P_z)$ on the lattice at a finite P_z and a UV scale of Λ and match it to the parton distribution $q(x, \mu)$ perturbatively where Λ will turn into the renormalization scale μ for the parton distribution at the infinite momentum frame (i.e. $P_z \to \infty$). Besides the perturbative matching from the quasiparton to the parton, this approach needs a renormalization procedure for the non-local operator which involves a spatial Wislon line to match the lattice results to those in the continuum. Furthermore, the hadron momentum P_z needs to be large. From the lattice calculation of $\tilde{q}(x, \Lambda, P_z)$ with $P_z \sim 1$ GeV [23, 24], it is found that the antiparton which is obtained from the negative x region, i.e. $\bar{q}(x) = -q(-x)$ is negative. This unphysical result is possibly due to the fact that $P_z \sim 1$ GeV is not large enough. This feature can be used to test how large a P_z is needed to have a positive probability for the CS part of the antipartons.

The present hadronic tensor approach requires calculation of 4-point functions on the lattice which is more numerically intensive than the large momentum approach which entails 3-point functions. Yet, it is simpler theoretically. There is no renormalization for the vector currents (other than the normalization to satisfy Ward identity for the non-conserved current on the lattice). Since $W_{\mu\nu}$ is Lorentz covariant, there is no need to work in the large momentum frame as in the large momentum approach. The frame independent W_1 and W_2 in $W_{\mu\nu}$ can be obtained with any hadron momentum. The most challenging part is to convert the Euclidean $\widetilde{W}_{\mu\nu}(\vec{q}, \vec{p}, \tau)$ to $W_{\mu\nu}(q^2, \nu)$ in Minkowski space. The improved MEM will be adopted to see how successful it is in this regard. Once the $W_{\mu\nu}(q^2, \nu)$ is obtained at the continuum and large volume limits and at the physical pion point, one can apply QCD factorization to fit the PDF to NNLO as is currently done in global fitting of the experimental lepton-hadron cross-sections. The advantage of having lattice results to supplement experimental data is that the flavors and the partons degrees of freedom, i.e. the valence, the CS and DS represented in Figs. 1(a), 1(b), and 1(c) are readily separated to better understand the role of each degree of freedom, their evolutions, as well as the flavor dependence.

References

[1] K. F. Liu and S. J. Dong, Phys. Rev. Lett. **72**, 1790 (1994), [hep-ph/9306299].

[2] K. F. Liu, S. J. Dong, T. Draper, D. Leinweber, J. H. Sloan, W. Wilcox and R. M. Woloshyn, Phys. Rev. D **59**, 112001 (1999) [hep-ph/9806491]

[3] K. F. Liu, Phys. Rev. D **62**, 074501 (2000), [hep-ph/9910306].

[4] U. Aglietti, M. Ciuchini, G. Corbo, E. Franco, G. Martinelli and L. Silvestrini, Phys. Lett. B **432**, 411 (1998), [hep-ph/9804416].

[5] W. Detmold and C. J. D. Lin, Phys. Rev. D **73**, 014501 (2006) [hep-lat/0507007].

[6] A. Airapetian *et al.* (HERMES Collaboration), Phys. Lett. **B666**, 446 (2008), [arXiv:0803.2993].

[7] H.L. Lai, M. Guzzi, J. Huston, Z. Li, P.M. Nadolsky, J. Pumplin, C.-P. Yuan, Phys. Rev. **D82**, 074024 (2010), [arXiv:1007.2241].

[8] T. Doi *et al.* (χ QCD Collaboration), PoS **LATTICE2008**, 163 (2008), [arXiv:0810.2482].

[9] K. F. Liu, W. C. Chang, H. Y. Cheng and J. C. Peng, Phys. Rev. Lett. **109**, 252002 (2012), [arXiv:1206.4339 [hep-ph]].

[10] G. S. Bali *et al.*, Phys. Rev. D **90**, no. 7, 074510 (2014), [arXiv:1408.6850 [hep-lat]].

[11] Y. B. Yang, A. Alexandru, T. Draper, M. Gong and K. F. Liu, Phys. Rev. D **93**, no. 3, 034503 (2016) [arXiv:1509.04616 [hep-lat]].

[12] W. Detmold, C. Lehner and S. Meinel, Phys. Rev. D **92**, no. 3, 034503 (2015), [arXiv:1503.01421 [hep-lat]].

[13] P. Hagler, B. U. Musch, J. W. Negele and A. Schafer, Europhys. Lett. **88**, 61001 (2009), [arXiv:0908.1283 [hep-lat]].

[14] B. U. Musch, P. Hagler, J. W. Negele and A. Schafer, Phys. Rev. D **83**, 094507 (2011), [arXiv:1011.1213 [hep-lat]].

[15] M. Engelhardt, B. Musch, P. Hägler, J. Negele and A. Schäfer, PoS CD **12**, 022 (2013).

[16] X. Ji, Phys. Rev. Lett. **110**, 262002 (2013), [arXiv:1305.1539 [hep-ph]].

[17] D. S. Roberts, W. Kamleh, D. B. Leinweber, M. S. Mahbub and B. J. Menadue, Phys. Rev. D **86**, 074504 (2012), doi:10.1103/PhysRevD.86.074504, [arXiv:1206.5891 [hep-lat]].

[18] M. Della Morte, B. Jaeger, T. Rae and H. Wittig, Eur. Phys. J. A **48**, 139 (2012), [arXiv:1208.0189 [hep-lat]].

[19] G. S. Bali, B. Lang, B. U. Musch and A. Schäfer, arXiv:1602.05525 [hep-lat].

[20] We thank X. Feng for pointing this out.

[21] R. Bryan, European Biophysics Journal, **18**, 165 (1990); M. Jarrell and J.E. Gubernatis, Phys. Rep. 269, 133 (1996).

[22] Y. Burnier and A. Rothkopf, Phys. Rev. Lett. **111**, 182003 (2013), [arXiv:1307.6106 [hep-lat]].

[23] H. W. Lin, J. W. Chen, S. D. Cohen and X. Ji, Phys. Rev. D **91**, 054510 (2015), [arXiv:1402.1462 [hep-ph]].

[24] C. Alexandrou, K. Cichy, V. Drach, E. Garcia-Ramos, K. Hadjiyiannakou, K. Jansen, F. Steffens and C. Wiese, Phys. Rev. D **92**, 014502 (2015), [arXiv:1504.07455 [hep-lat]].